Decision between mitophagy and apoptosis by Parkin via VDAC1 ubiquitination

Su Jin Ham[a,b,1], Daewon Lee[b,c,1], Heesuk Yoo[a,b], Kyoungho Jun[b,c], Heejin Shin[b], and Jongkyeong Chung[a,b,c,2]

[a]Interdisciplinary Graduate Program in Genetic Engineering, Seoul National University, 08826 Seoul, Republic of Korea; [b]Institute of Molecular Biology and Genetics, Seoul National University, 08826 Seoul, Republic of Korea; and [c]School of Biological Sciences, Seoul National University, 08826 Seoul, Republic of Korea

Edited by Norbert Perrimon, Harvard Medical School, Boston, MA, and approved January 22, 2020 (received for review June 10, 2019)

VDAC1 is a critical substrate of Parkin responsible for the regulation of mitophagy and apoptosis. Here, we demonstrate that VDAC1 can be either mono- or polyubiquitinated by Parkin in a PINK1-dependent manner. VDAC1 deficient with polyubiquitination (VDAC1 Poly-KR) hampers mitophagy, but VDAC1 deficient with monoubiquitination (VDAC1 K274R) promotes apoptosis by augmenting the mitochondrial calcium uptake through the mitochondrial calcium uniporter (MCU) channel. The transgenic flies expressing *Drosophila* Porin K273R, corresponding to human VDAC1 K274R, show Parkinson disease (PD)-related phenotypes including locomotive dysfunction and degenerated dopaminergic neurons, which are relieved by suppressing MCU and mitochondrial calcium uptake. To further confirm the relevance of our findings in PD, we identify a missense mutation of Parkin discovered in PD patients, T415N, which lacks the ability to induce VDAC1 monoubiquitination but still maintains polyubiquitination. Interestingly, *Drosophila* Parkin T433N, corresponding to human Parkin T415N, fails to rescue the PD-related phenotypes of *Parkin*-null flies. Taken together, our results suggest that VDAC1 monoubiquitination plays important roles in the pathologies of PD by controlling apoptosis.

apoptosis | VDAC1 | Parkin | Parkinson disease | PINK1

Parkinson disease (PD) is a neurodegenerative disease caused by the selective loss of dopaminergic (DA) neurons in the substantia nigra of the brain. Its symptoms include tremor, rigidity and dyskinesia (1). A series of genetic studies has identified a group of genes associated with the pathogenesis of PD such as *SNCA* (α-synuclein), *PARK2* (Parkin), *PARK6* (PINK1), *PARK7* (DJ-1), and *PARK8* (*LRRK2*) (2–7).

Among the PD-associated genes mentioned above, *PARK6* encodes PTEN-induced putative kinase1 (PINK1) and *PARK2* encodes Parkin, which is a RING/HECT type E3 ubiquitin ligase. Parkin is phosphorylated at serine 65 located within the ubiquitin-like (UBL) domain by PINK1 and then its E3 ligase activity is activated (8, 9). PINK1 is a serine/threonine kinase that is activated under mitochondrial damages. For example, the mitochondrial depolarization resulting from carbonyl cyanide *m*-chlorophenyl hydrazine (CCCP) treatment accumulates PINK1 on the surface of damaged mitochondria and sequentially activates and translocates Parkin to mitochondria from the cytosol (10–12). Parkin is localized to the mitochondria and then ubiquitinates multiple substrates, including mitofusin1 (MFN1), mitofusin2 (MFN2), translocase of outer membrane20 (TOM20), mitochondrial Rho GTPase1 (Miro1), and voltage-dependent anion-selective channel 1 (VDAC1) (13–15). Through controlling these mitochondrial proteins, the PINK1–Parkin pathway plays critical roles in maintaining mitochondrial homeostasis by regulating mitophagy, mitochondrial dynamics, and mitochondria-mediated apoptosis.

VDAC1 is a protein anchored in the outer mitochondrial membrane and forms a pore with a beta-barrel structure consisting of 19 beta-strands (16). VDAC1 functions as a critical component of mitochondrial permeability transition pore (mPTP), by forming a complex with cyclophilin D (CypD) from the mitochondrial matrix and adenine nucleotide translocase (ANT) from the inner mitochondrial membrane, and transports small molecules including metabolites, calcium, and cytochrome *c* (17–22). When Parkin induces polyubiquitination on VDAC1, the ubiquitinated VDAC1 triggers Parkin-mediated mitophagy by recruiting p62/sequestosome1 (SQSTM1) and LC3B to the mitochondria (23). VDAC1 also regulates apoptosis by controlling the opening and closing of its pore. According to previous studies, anti-apoptotic proteins such as β-cell lymphoma 2 (Bcl-2) and Bcl-extralarge (Bcl-xL) or hexokinase1 (HK1) and hexokinase2 (HK2) inhibit apoptosis by binding to VDAC1, shutting down the cytosolic transportation of apoptotic signaling molecules including cytochrome *c* (24–27). On the contrary, proapoptotic proteins such as Bcl-2–associated X protein (Bax) and Bax-like BH3 protein (BID) bind to VDAC1 and open VDAC1 pore, hence releasing cytochrome *c* to the cytosol (18, 28, 29). In addition, the self-oligomerization of VDAC1 has been reported to regulate apoptosis by controlling the release of apoptotic signaling molecules to the cytosol (30). Furthermore, VDAC1-mediated mitochondrial calcium influx is an important mechanism in regulating apoptosis. VDAC1 binds to the endoplasmic reticulum (ER)-localized inositol trisphosphate receptor (IP_3R) and glucose-regulated protein75 (Grp75), tethering mitochondria to the ER and forming mitochondria-associated ER membrane (MAM) (31). This suggests that increases in calcium level in the ER or in the cytosol induce VDAC1-mediated calcium

Significance

VDAC1 transports ions and small molecules at the mitochondrial outer membrane. In this study, we discover that Parkin, a frequently mutated Parkinson disease protein, ubiquitinates VDAC1 in two different manners, poly- and monoubiquitination. Interestingly, VDAC1 defective in polyubiquitination hinders Parkin-mediated mitophagy, but VDAC1 defective in monoubiquitination induces apoptosis. When VDAC1 deficient with monoubiquitination is expressed in mammalian cells and fruit fly, we observe increased mitochondrial calcium influx and apoptosis and typical in vivo phenotypes related to Parkinson disease, such as defective locomotive activity and loss of dopaminergic neurons. These results suggest that the dual regulation of mitophagy and apoptosis by Parkin via VDAC1 poly- and monoubiquitination is highly critical in protecting cells from the pathogenesis of Parkinson disease.

Author contributions: S.J.H. and J.C. designed research; S.J.H., D.L., H.Y., K.J., and J.C. performed research; S.J.H., D.L., H.Y., K.J., and J.C. contributed new reagents/analytic tools; S.J.H., D.L., H.Y., and J.C. analyzed data; and S.J.H., D.L., H.S., and J.C. wrote the paper.

The authors declare no competing interest.

This article is a PNAS Direct Submission.

[1]S.J.H. and D.L. contributed equally to this work.

[2]To whom correspondence may be addressed. Email: jkc@snu.ac.kr.

This article contains supporting information online at https://www.pnas.org/lookup/suppl/doi:10.1073/pnas.1909814117/-/DCSupplemental.

First published February 11, 2020.

transport into the mitochondria. Mitochondrial calcium uniporter (MCU) in the inner mitochondrial membrane directly interacts with VDAC1 and plays a crucial role in mediating calcium flux all of the way into the matrix of the mitochondria (32). A rise in calcium influx causes mitochondria swelling, eventually rupturing the outer mitochondrial membrane and releasing cytochrome *c* into the cytosol to trigger apoptosis (22, 33).

The mitophagy induced by PINK1 and Parkin is mediated by adaptor proteins that have ubiquitin-binding motifs and LC3B-binding motifs (LIR). The ubiquitinated substrates of Parkin in the mitochondria recruit adaptor proteins, such as p62/SQSTM1, neighbor of BRCA1 (NBR1), NDP52, optineurin (OPTN), and Tax1-binding protein1 (TAX1BP1) (23, 34–36). Recruitment of these adaptor proteins promotes formation of autophagosome on the mitochondria and ultimately induces selective degradation of mitochondria in the lysosome. Furthermore, the PINK1–Parkin pathway is also responsible for regulating apoptosis. Particularly in *Drosophila* models, PINK1 and Parkin knockdown or knockout (KO) mutants display significant features related to apoptosis such as increased apoptosis, muscle degeneration, loss of DA neurons, and increased sensitivity to mitochondrial damages (37). Importantly, these phenotypes can be rescued by expressing the anti-apoptotic protein Bcl-2, suggesting that increased apoptosis in PINK1 and Parkin mutants is critical in inducing PD pathogenesis (37). These biochemical and genetic data consistently support the importance of mitophagy and apoptosis in PD pathogenesis, but the relationship between two different self-destructive mechanisms regulated by the PINK1–Parkin pathway remains unclear. Hence, we have decided to investigate the possibility of the PINK1–Parkin pathway controlling a common substrate, which regulates mitophagy and apoptosis simultaneously.

In this study, we have discovered that the PINK1–Parkin pathway controls both mitophagy and apoptosis by inducing two different types of ubiquitination on VDAC1. The polyubiquitinated VDAC1 regulates Parkin-mediated mitophagy, whereas the monoubiquitinated VDAC1 regulates mitochondrial calcium uptake, which ultimately protects cells from apoptosis. We have additionally observed that the Parkin T415N PD patient mutant fails to induce VDAC1 monoubiquitination. Consistent with these mammalian data, the transgenic flies expressing *Drosophila* Porin or Parkin defective in VDAC/Porin monoubiquitination display the phenotypes related to PD, supporting the critical role of apoptosis in the pathogenesis of PD.

Results

Mono- and Polyubiquitination of VDAC1 Are Dependent on PINK1 and Parkin but Occur Independently from Each Other. VDAC1 is a critical mitochondrial substrate for Parkin that mediates mitophagy and apoptosis under mitochondrial damages (23). To investigate the regulatory mechanism of VDAC1 by Parkin, we examined VDAC1 ubiquitination in the presence of wild-type (WT) Parkin or an E3 activity-dead Parkin C431S (CS) when cells were treated with CCCP in HEK293T cells. As expected, VDAC1 was polyubiquitinated in the presence of Parkin WT but not in the cells expressing Parkin CS (Fig. 1*A*). Intriguingly, an unexpected ∼42-kDa ubiquitinated VDAC1 protein band, which corresponds to the molecular weight of VDAC1 with monoubiquitination, appeared when VDAC1 and Parkin WT were coexpressed (Fig. 1*A*). Similarly, we observed monoubiquitinated endogenous VDAC1 in HEK293T cells upon CCCP treatment when Parkin WT was expressed (*SI Appendix*, Fig. S1*A*). To confirm whether this ubiquitinated band contains monoubiquitination, we employed a K0-ubiquitin mutant in which all lysine residues of ubiquitin were substituted with arginines, allowing for only monoubiquitination to occur. When K0-ubiquitin was expressed, the polyubiquitination of VDAC1 was substantially inhibited, but the ∼42-kDa band remained intact (Fig. 1*B*). These results confirmed that Parkin induces both mono- and polyubiquitination of VDAC1 and that these two different types of VDAC1 ubiquitination occur independently from each other.

Next, we identified lysine residues in VDAC1 that were conserved across different species to search for the sites of poly- and monoubiquitination. We aligned the VDAC1 protein sequences over various animal species, including *Homo sapiens*, *Arabidopsis thaliana*, *Rattus norvegicus*, *Mus musculus*, and *Drosophila melanogaster* (Fig. 1*C*). Based on this, we generated VDAC1 mutants that substituted the conserved lysine residues with arginines and performed ubiquitination assays with them in HEK293T cells. As a result, we found the lysine residues that corresponded to two different states of VDAC1 ubiquitination: lysine 274 (K274) for VDAC1 monoubiquitination and lysines 12, 20, 53, 109, and 110 (Poly-K) for VDAC1 polyubiquitination (Fig. 1*C*). In order to verify whether these lysine residues can actually be ubiquitinated, we determined the three-dimensional locations of the ubiquitinated lysine residues in human VDAC1 protein (Fig. 1*C*). Interestingly, the lysine residues of VDAC1 were not embedded in the transmembrane hydrophobic region but rather were located at the exposed cytosolic domain of the protein, confirming the accessibility of the residues to Parkin E3 ligase.

To confirm the Parkin-dependent mono- and polyubiquitination on VDAC1, we transfected HeLa cells lacking endogenous Parkin protein with HA-tagged VDAC1 WT, K274R, or polyubiquitination-defective mutant (henceforth, Poly-KR) generated through substitution of Poly-K with arginines. These cells were cotransfected with Parkin WT or CS and were treated with CCCP (Fig. 1*D*). Strikingly, we observed that VDAC1 monoubiquitination was completely abolished in VDAC1 K274R without significant changes in its polyubiquitination (Fig. 1*D*). However, VDAC1 Poly-KR maintained its monoubiquitination with highly diminished polyubiquitination (Fig. 1*D*).

In our previous study, we established that PINK1 is an upstream regulator of Parkin. Hence, to confirm whether VDAC1 ubiquitination is regulated by the kinase activity of PINK1, we performed ubiquitination assays of VDAC1 WT, K274R, and Poly-KR in HEK293T cells expressing PINK1 WT or a kinase-dead form of PINK1 mutant (KD; K219A/D362A/D384A). As expected, PINK1 also selectively induced poly- and monoubiquitination on VDAC1 K274R and Poly-KR, respectively, in a kinase activity-dependent manner (*SI Appendix*, Fig. S1*B*). These results allowed us to conclude that both mono- and polyubiquitination of VDAC1 depend on the PINK1–Parkin signaling pathway.

Mono- and Polyubiquitination of VDAC1 Determine the Occurrence of Apoptosis and Mitophagy. Having shown that VDAC1 is either poly- or monoubiquitinated by Parkin, we sought to examine the functional roles of both types of ubiquitination in mitochondria-related physiologies such as mitophagy and apoptosis. According to previous reports, Parkin-mediated mitophagy occurs when various mitochondrial proteins, including VDAC1, are ubiquitinated and p62/SQSTM1 proteins are recruited (13, 23). In order to detect mitophagy, we expressed VDAC1 WT, K274R, Poly-KR, or All-KR (the combined mutant for K274R and Poly-KR) in VDAC1 KO mouse embryonic fibroblast (MEF) cells coexpressing Parkin to observe the recruitment of p62/SQSTM1 to the mitochondria under CCCP treatment. Interestingly, the expression of VDAC1 Poly-KR or All-KR in VDAC1 KO cells strongly hindered the recruitment of p62/SQSTM1 to the mitochondria when treated with CCCP, compared to the cells expressing VDAC1 WT or K274R (Fig. 2*A*). According to the quantification analysis, over 80% of VDAC1 WT or K274R-expressing cells showed colocalization of p62/SQSTM1 with the mitochondria when treated with CCCP (Fig. 2*B*). In contrast, the percentage of cells with p62/SQSTM1 in

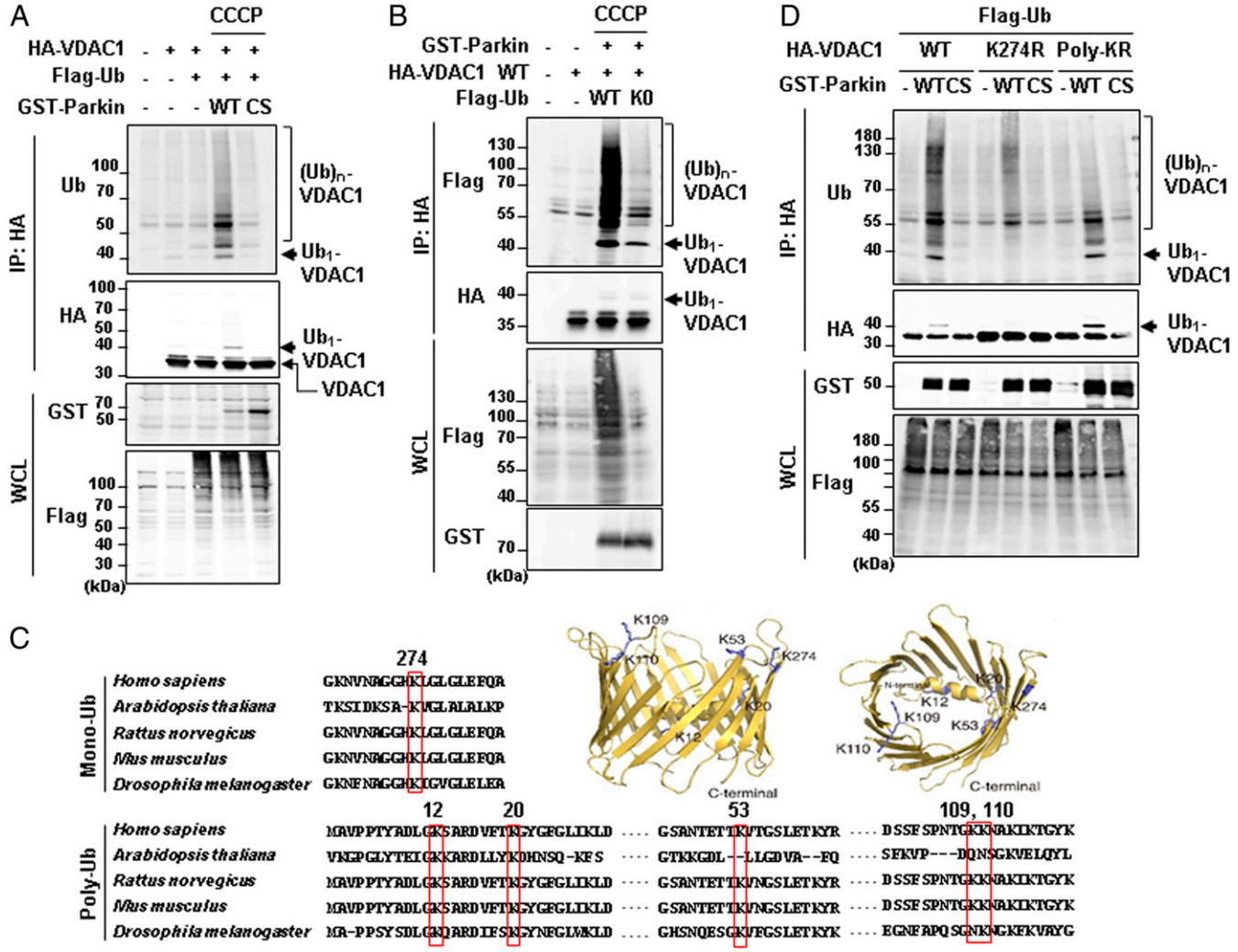

Fig. 1. Mono- and polyubiquitination of VDAC1 are dependent on Parkin and PINK1 activity. (*A*, *B*, and *D*) Ubiquitination assays for VDAC1 by Parkin. HEK293T cells were transfected with indicated constructs and treated with or without 20 μM CCCP for 4 h. Whole-cell lysates (WCL) were immunoprecipitated (IP) and analyzed for IB analyses with indicated antibodies. The monoubiquitination band was marked on the right side and the polyubiquitination bands were marked by a bracket. Parkin WT and CS (C431S) mutants were expressed and compared in *A* and *D*. Flag-tagged ubiquitin WT and K0 (K6, 11, 27, 29, 33, 48, and 63R mutant) were expressed in *B*. VDAC1 WT and two ubiquitination mutants (VDAC1 K274R and Poly-KR) were expressed and also examined for Parkin-dependent ubiquitination assays in *D*. (*C*) Aligned VDAC1 protein sequences of human (VDAC1, P21796.2), *Arabidopsis* (VDAC1, NP_186777.1), rat (VDAC1, NP_112643.1), mouse (VDAC1 isoform 2, NP_035824.1), and *Drosophila* (Porin isoform E, NP_001260365.1) with indication of the conserved lysine residues in red boxes. Three-dimensional human VDAC1 protein structures, Protein Data Bank ID code 5JDP (P21796), were additionally used to predict the location of mono- and polyubiquitination sites.

the mitochondria was decreased to ~40% in VDAC1 Poly-KR– or All-KR–expressing cells (Fig. 2*B*). Consistent with these immunocytochemistry data, immunoblot (IB) analyses also showed that CCCP treatment significantly decreased the amount of mitochondrial proteins in the outer membrane (MFN1 and TOM20) and inner membrane (COXIV, NDUFS3, and TIM23) of VDAC1 WT or K274R-expressing cells (Fig. 2*C*). In comparison, VDAC1 Poly-KR– or All-KR–expressing cells did not display decreased mitochondrial protein levels (Fig. 2*C*). These results indicated that VDAC1 polyubiquitination is critical for PINK1 and Parkin-mediated mitophagy.

Bax, a member of Bcl-2 family, is a proapoptotic protein that exists in an inactive form in the cytosol of healthy cells. However, in response to apoptotic stimuli, Bax undergoes a conformational change and is inserted into the outer mitochondrial membrane, where it is oligomerized (38–40). As a result, cytochrome *c* is released from the mitochondria to the cytosol, which activates Apaf1 and caspase cascades (41). Apoptosis triggered by activated caspases induces PARP protein cleavage and ultimately mitochondria-mediated cell death (42). As previous studies showed that VDAC1 also regulates the apoptosis process, we hypothesized that VDAC1 K274 monoubiquitination may regulate apoptosis. To visualize the apoptotic status affected by the expression of VDAC1 WT, K274R, Poly-KR, or All-KR, we observed Bax localization in the mitochondria of HeLa cells that were stably expressing GFP-Parkin. As a result, we observed that the cells expressing VDAC1 K274R or All-KR displayed a significant increase in Bax translocation to the mitochondria, compared to HeLa cells expressing VDAC1 WT or Poly-KR (Fig. 2*D*). Quantitative analysis revealed that about 20% of the cells showed translocation of Bax to the mitochondria when VDAC1 K274R or All-KR was expressed. However, in the cells expressing VDAC1 WT or Poly-KR mutant, Bax localization in the mitochondria was rare, if not detected (Fig. 2*E*). Furthermore, we performed IB analyses for cleaved PARP as an apoptosis marker. Dose-dependent expression of VDAC1 WT,

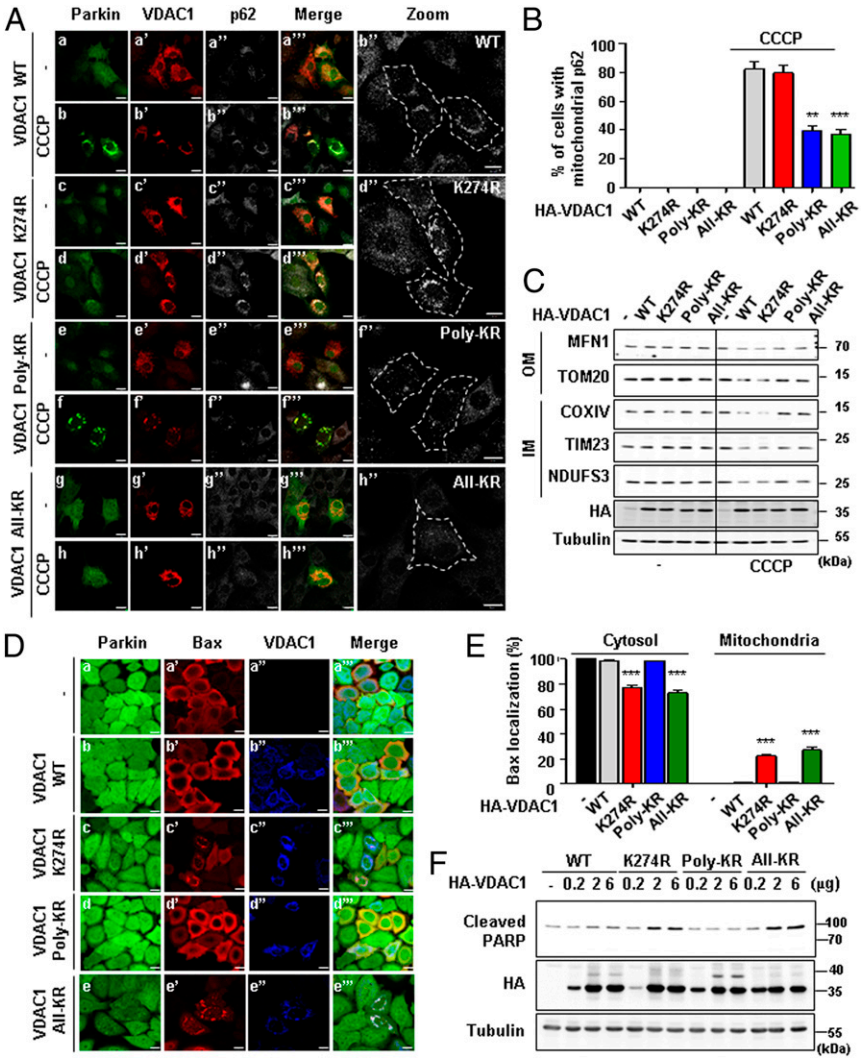

Fig. 2. Poly- and monoubiquitination on VDAC1 determine the fate of mitochondria to mitophagy or apoptosis, respectively. (*A*) Confocal images of the translocation of p62/SQSTM1 to mitochondria. VDAC1 KO MEF cells were transfected with HA-tagged VDAC1 WT, K274R, Poly-KR, or All-KR and treated with 30 μM CCCP for 8 h. Subcellular localizations of YFP-Parkin (green), VDAC1 (red), and p62/SQSTM1 (gray) were observed. (Scale bars, 20 μm.) (*B*) Percentage of the cells with p62/SQSTM1 localized to the mitochondria in *A* ($n > 500$ cells from three independent experiments). Data were analyzed by ANOVA Tukey test. $^{**}P < 0.01$; $^{***}P < 0.001$. (*C*) Concentrations of mitochondrial proteins from the outer membrane (OM) and inner membrane (IM) in VDAC1 KO MEF cells with indicated VDAC1 proteins transfected for 48 h and treated with or without 30 μM CCCP for 16 h. (*D*) Confocal images of Bax translocated to the mitochondria. Subcellular localizations of GFP-Parkin (green), Bax (red), and VDAC1 proteins (blue) were observed. (Scale bars, 20 μm.) (*E*) Percentage of the cells with Bax localized to mitochondria in *D* ($n > 500$ cells from three independent experiments). Data were analyzed by one-way ANOVA with Tukey multiple-comparison test and are presented as means ± SD. $^{***}P < 0.001$. (*F*) HeLa cells stably expressing GFP-Parkin were transfected with indicated VDAC1 proteins in a dose-dependent manner and analyzed by immunoblotting to examine indicated proteins.

K274R, Poly-KR, or All-KR in HeLa cells stably expressing GFP-Parkin revealed that PARP cleavage was increased in correlation with VDAC1 K274R or All-KR expressions (Fig. 2*F*). However, VDAC1 WT or Poly-KR expression did not induce such changes in PARP cleavage (Fig. 2*F*), suggesting that VDAC1 with K274 monoubiquitination inhibits apoptosis. Taken together with the aforementioned data, we concluded that Parkin controls apoptosis and mitophagy via mono- and polyubiquitination of VDAC1, respectively.

Monoubiquitination-Deficient VDAC1 Mutant Induces Apoptosis by Augmenting Mitochondrial Calcium Uptake. VDAC1 is a route for mitochondrial calcium uptake and the increased mitochondrial calcium changes diverse mitochondrial homeostasis (43). To observe the change in mitochondrial morphology, we performed electron microscopy (EM) analysis of VDAC1 WT or K274R-expressing HeLa cells that were stably expressing GFP-Parkin. In our observation, cells expressing VDAC1 K274R displayed swelled mitochondria with defective cristae structures (*SI Appendix*, Fig. S2).

Considering the prior results, we hypothesized that VDAC1 monoubiquitination may regulate apoptosis in cells by changing mitochondrial calcium uptake. To test this hypothesis, we measured the level of mitochondrial calcium uptake using 4mitD3 (458 nm excitation/470 to 500 and 530 to 560 nm emission) as a calcium indicator. We expressed VDAC1 WT or K274R with 4mitD3 in VDAC1 KO MEF cells to see the change in the ratio of green and red fluorescence. Notably, cells expressing VDAC1 K274R exhibited an increase in mitochondrial calcium uptake more than cells expressing VDAC1 WT (Fig. 3*A*). Quantification analyses on the maximum response of the calcium uptake further substantiated the significant increase in calcium uptake in cells expressing VDAC1 K274R compared

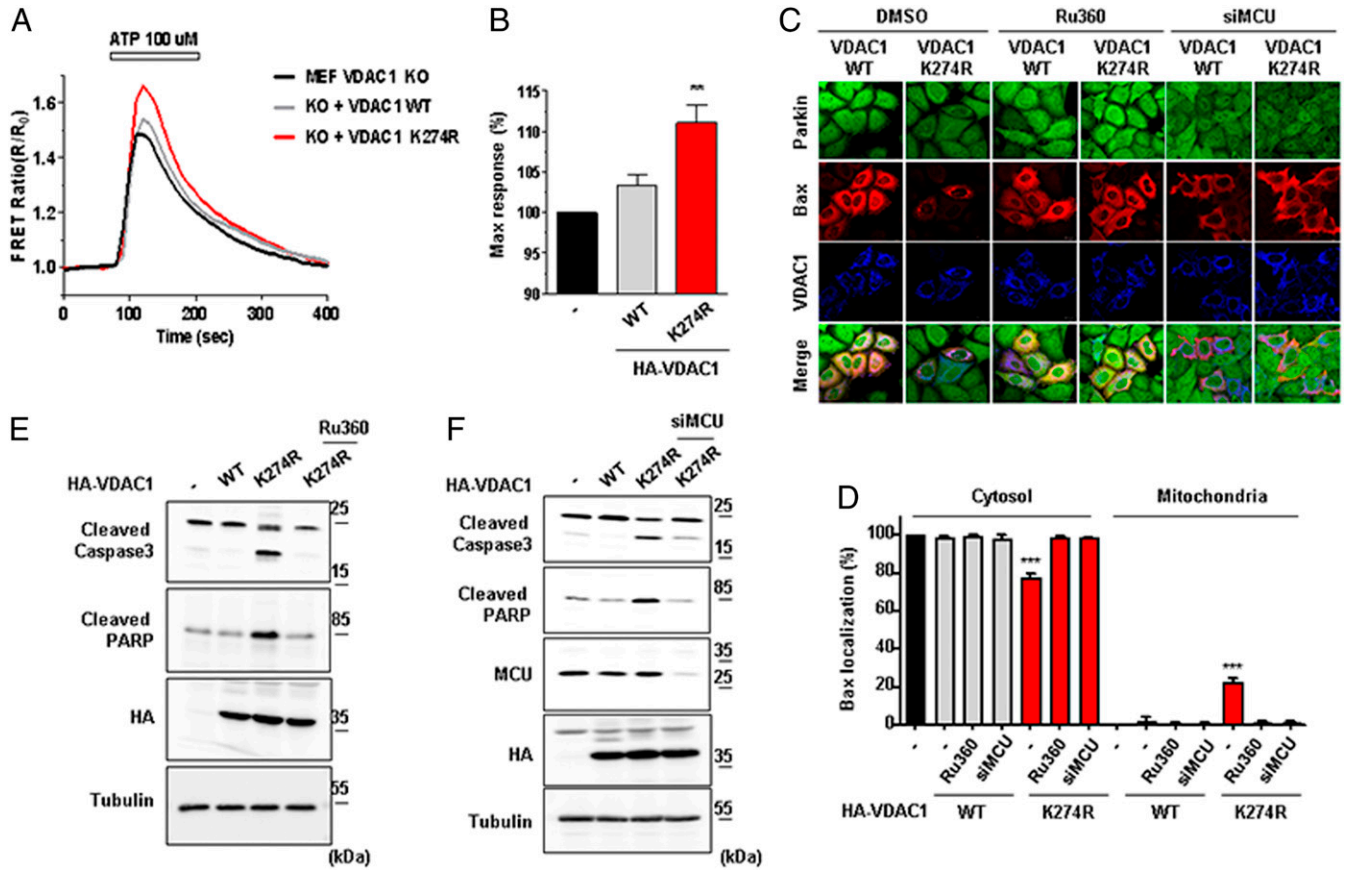

Fig. 3. Monoubiquitination-deficient VDAC1 induces apoptosis by increasing mitochondrial calcium uptake. (*A* and *B*) Mitochondrial calcium dynamics in VDAC1 KO MEF cells. VDAC1 KO MEF cells were transfected with HA-tagged VDAC1 WT or K274R and cotransfected with 4mitD3, a mitochondrial calcium indicator, for 48 h. Cells were then treated with 100 μM ATP for 3 min and were monitored for the changes in 4mitD3 fluorescence. (*B*) Maximum mitochondrial calcium uptake for VDAC1 KO MEF cells expressing VDAC1 WT or K274R in *A*. All of the values were normalized to the basal level of VDAC1 KO MEF cells transfected with empty vector (–) (n = 50 to ~70 cells). Data were analyzed by ANOVA Tukey test. $^{**}P < 0.05$. (*C* and *D*) Confocal images of Bax translocated to the mitochondria. (*C*) Flag-tagged Bax (red) and HA-tagged VDAC1 WT or K274R (blue) were transfected and immune-stained with Flag and HA antibodies in HeLa cells stably expressing GFP-Parkin (green). Cells were treated with or without 0.5 mM Ru360 for 8 h or transfected with MCU siRNA. (Scale bars, 20 μm.) (*D*) Percentage of cells with Bax localized in the cytosol or the mitochondria shown in *C* (n > 500 cells from three independent experiments). Data were analyzed by one-way ANOVA with Tukey multiple-comparison test and are presented as means ± SD. $^{***}P < 0.001$. (*E* and *F*) HA-tagged VDAC1 WT or K274R was transfected in HeLa cells stably expressing GFP-Parkin. Cells were treated with or without 0.5 mM Ru360 for 8 h in *E* or transfected with MCU siRNA in *F*. Cell lysates were analyzed by immunoblotting to examine indicated proteins.

to VDAC1 WT (Fig. 3*B*). We also tested mitochondrial calcium uptake in cells expressing VDAC1 Poly-KR. In contrast, there was no significant mitochondrial calcium influx difference between cells expressing VDAC1 WT and cells expressing VDAC1 Poly-KR (*SI Appendix*, Fig. S3 *A* and *B*).

To confirm the involvement of calcium, we suppressed mitochondrial calcium uptake using a mitochondrial calcium uptake inhibitor, Ru360, and MCU small interfering RNA (siRNA). We expressed HA-tagged VDAC1 WT or K274R and Flag-tagged Bax in HeLa cells stably expressing GFP-Parkin and treated with Ru360 or MCU siRNA. Confocal images showed that Bax was translocated from the cytosol to the mitochondria only in VDAC1 K274R-expressing cells, and this mitochondrial translocation of Bax was nearly blocked by Ru360 or MCU siRNA (Fig. 3*C*). In quantitative analyses, ~21% of VDAC1 K274R-expressing cells showed mitochondrial translocation of Bax, while only 1 to 2% was observed in the Ru360- or MCU siRNA-treated cells (Fig. 3*D*). For further examination, we analyzed the amount of cleaved PARP and caspase3 with or without the treatment of Ru360 or MCU siRNA in the same experimental set. As anticipated, PARP and caspase 3 cleavage induced by VDAC1 K274R expression significantly decreased when cells were treated with Ru360 (Fig. 3*E*) or MCU siRNA (Fig. 3*F*). However, VDAC1 WT or Poly-KR expression did not induce such apoptotic changes in caspase3 cleavage (*SI Appendix*, Fig. S3*C*). These data supported that the loss of monoubiquitination on VDAC1 induces apoptotic processes by increasing mitochondrial calcium uptake.

Porin Mutants with Defective Ubiquitination Induce Locomotor Defects, Apoptosis, and Neurodegeneration. To confirm our cell biology results in vivo, we generated transgenic flies expressing Porin (the *Drosophila* ortholog of human VDAC1) WT, K273R (corresponding to human VDAC1 K274R), or Poly-KR (lysine 12, 20, 53, and 110 to arginines). Among the polyubiquitinated lysine residues in human VDAC1, the lysine 109 site is not conserved in *Drosophila*. Initially, we quantified the expression of Porin WT, K273R, or Poly-KR in the transgenic flies through immunoblotting to confirm that they were similarly expressed (*SI Appendix*, Fig. S4*A*). Also, we conducted ubiquitination assays for Porin in HEK293T cells and Schneider 2 (S2) cells and observed that Porin mono- and polyubiquitination by Parkin occurred in a highly conserved manner (*SI Appendix*, Fig. S5 *A* and *B*). We therefore expressed Porin mutant proteins in fly muscles using the *Mef2-Gal4* driver and analyzed wing postures and muscle apoptosis. To

identify apoptosis in vivo, we performed terminal deoxynucleotidyl transferase deoxyuridine triphosphate nick-end labeling (TUNEL) assays in the thorax muscle of 3-d-old flies. In our findings, over 40% of Porin K273R flies displayed abnormal wing postures, whereas less than 20% of Porin WT or Poly-KR flies displayed the phenotype (Fig. 4 *A* and *B*). Moreover, TUNEL assays showed that apoptosis was highly increased in Porin K273R transgenic flies (~80%) compared to Porin WT or Poly-KR flies (~20 to 30%) (Fig. 4 *C* and *D*). In addition, to examine whether VDAC1 ubiquitination affects locomotive ability of the transgenic flies, we performed climbing assays for Porin WT, K273R, and Poly-KR flies. As a result, Porin K273R flies showed impaired climbing ability compared to Porin WT or Poly-KR transgenic flies (Fig. 4*E*). Finally, we observed the loss of DA neurons in the Porin transgenic flies under the control of *TH-gal4* driver, which induces Porin expression in DA neurons. When we counted the number of DA neurons in the protocerebral posterior lateral 1 (PPL1) of *Drosophila* adult brain, Porin K273R transgenic flies displayed significant decreased DA neurons, while Porin WT or Poly-KR transgenic flies were observed to have similar neuron numbers compared to the control flies (Fig. 4*F* and *SI Appendix*, Fig. S7*A*). In summary, these *Drosophila* results demonstrated that VDAC1 deficient with monoubiquitination increases apoptosis in vivo and also induces PD-related phenotypes, such as defective locomotive activity and loss of DA neurons. Furthermore, we discovered that all defective phenotypes of Porin K273R transgenic flies were almost completely rescued by deletion of MCU mitochondrial calcium channel (Fig. 4 *A*–*F*).

In addition, we generated All-KR (K12R, K20R, K53R, K110R, and K273R) transgenic flies and observed wing posture, apoptotic signal, climbing ability, and DA neurons. As expected, Porin All-KR mutant flies displayed abnormal wing postures and increased apoptotic signals in thoraces (*SI Appendix*, Fig. S6 *A*–*D*). In addition, Porin All-KR flies displayed significant decreases in climbing ability and DA neurons (*SI Appendix*, Figs. S6 *E* and *F* and S7*A*). Compared to Porin K273R or Poly-KR flies, Porin All-KR flies showed combined phenotypes between Porin K274R and Poly-KR flies (*SI Appendix*, Fig. S6 *A*–*F*).

Furthermore, to determine whether endogenous Porin proteins affect the phenotypes, we generated transgenic flies expressing Porin WT, K273R, Poly-KR, or All-KR in a Porin KO

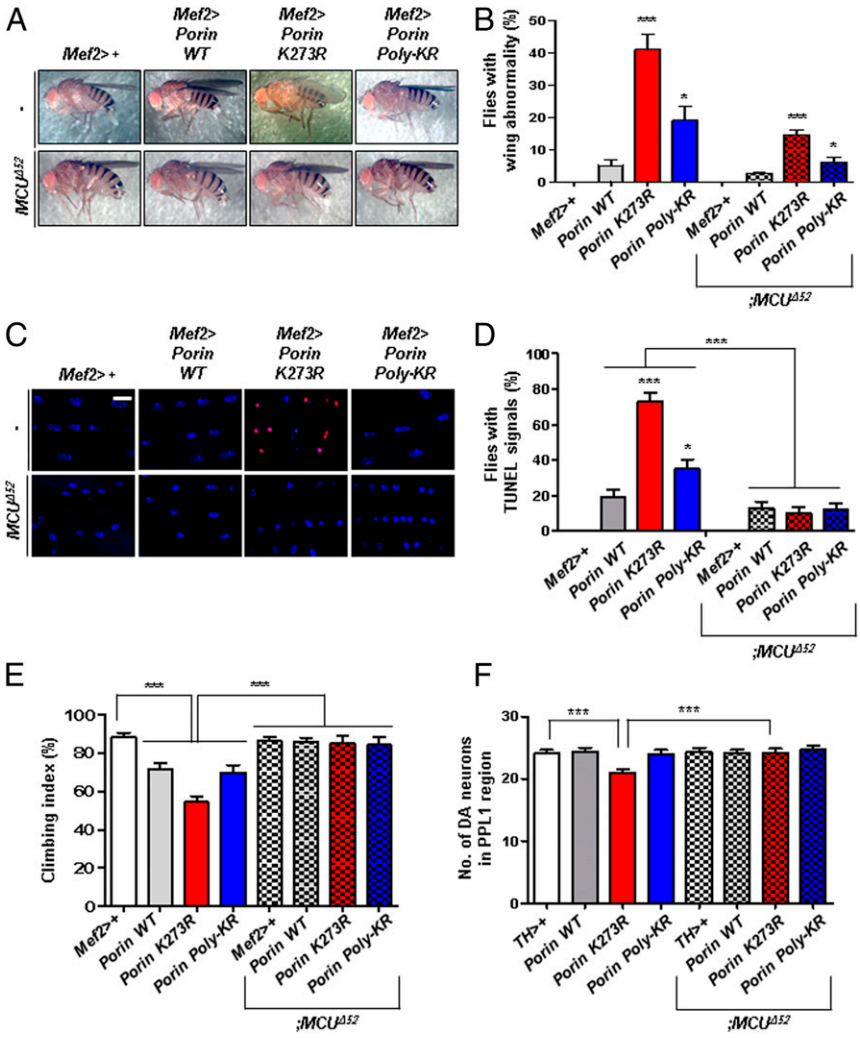

Fig. 4. All phenotypes related to PD in Porin K273R flies are rescued by suppressing MCU. (*A* and *B*) Defects in the wing posture of Porin K273R flies. Transgenic flies expressing Porin WT, K273R, or Poly-KR using *Mef2-Gal4* driver were crossed with MCU null flies ($MCU^{\Delta 52}$). (*B*) Percentage of the flies with defective wing postures in *A* ($n = 300$ from three independent experiments). (*C* and *D*) TUNEL signals for apoptosis (red) and 4′,6-diamidino-2-phenylindole staining for the nucleus (blue) in the thoraces of transgenic flies. (Scale bar, 5 μm.) (*D*) Percentage of the flies with TUNEL signals in *C* ($n = 100$ from 10 independent experiments). (*E*) Percentage of the transgenic flies with defective climbing ability ($n = 100$ from 10 independent experiments). (*F*) Numbers of DA neurons in the brain PPL1 region ($n = 10$). All quantifications were analyzed by one-way ANOVA with Tukey multiple-comparison test and are presented as means ± SD. ***$P < 0.001$; *$P < 0.05$.

background ($Porin^{A2}$) (44). In $Porin^{A2}$ mutant flies, the climbing ability was slightly decreased, but apoptosis in thoraces, wing abnormalities, and DA neuron numbers were similar to those of the control flies (*SI Appendix*, Figs. S6 and S7*B*). When we generated transgenic flies, each phenotype of Porin WT, K273R, Poly-KR, or All-KR flies in the $Porin^{A2}$ background was statistically similar to that of Porin WT, K273R, Poly-KR, or All-KR flies in the WT background (*SI Appendix*, Figs. S6 and S7*B*).

Taken together, we concluded that the Porin mutants lacking mono- and/or polyubiquitination on VDAC1 induces PD-related phenotypes in *Drosophila*.

Parkin T415N PD Patient Mutant Fails to Induce VDAC1 Monoubiquitination. To determine whether the pathogenesis of PD can be induced by impairing the regulatory mechanism of VDAC1 monoubiquitination in PD patients, we performed VDAC1 ubiquitination assays for Parkin with PD patient mutations. The UBL domain in the N terminus and the RING0, RING1, in-between-ring (IBR), and RING2 domains in the C terminus are important domains for the E3 ligase activity of Parkin, and thus mutations in these domains are expected to be critical for the pathogenesis of PD (Fig. 5*A*). A total of 63 missense mutations were generated in Parkin (Fig. 5*A*), and we measured their activities in inducing VDAC1 mono-ubiquitination compared to that of Parkin WT in HEK293T cells

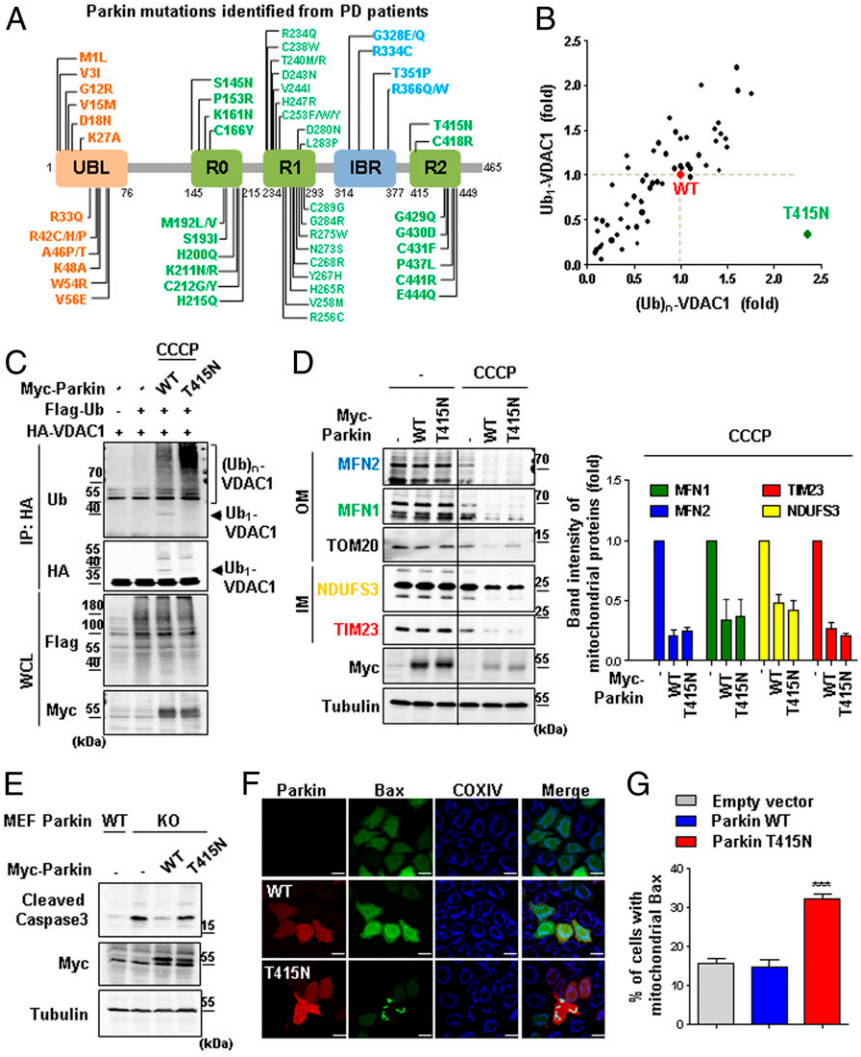

Fig. 5. Impaired monoubiquitination of VDAC1 by Parkin T415N leads to apoptosis. (*A*) Parkin PD patient mutations in the domains of Parkin protein. Listing from the N-terminal to the C-terminal region, Parkin consists of UBL, really-interesting-new-gene (RING) 0, RING1, in-between RING (IBR), and RING2 domains. (*B*) Summarized results of the ubiquitination assays for VDAC1 by 63 different Parkin PD patient mutants. Mono- and polyubiquitination activities of these Parkin mutants were normalized to the mono- and polyubiquitination of VDAC1 by Parkin WT (red). The Parkin T415N mutant (green) showed significant reduction in the monoubiquitination of VDAC1. We quantitated band intensities of ubiquitination on VDAC1 using Image J program. (*C*) Ubiquitination assays on the Parkin T415N mutant. Monoubiquitination of VDAC1 is indicated by arrows, and the bracket represents the polyubiquitination. IP, immunoprecipitated; WCL, whole-cell lysates. (*D*) Mitochondrial proteins analyzed by immunoblotting. HeLa cells were expressed with Myc-tagged Parkin WT or T415N with or without 20 μM CCCP for 12 h. A quantitation graph shows the protein band intensity of MFN2 (blue), MFN1 (green), NDUFS3 (yellow), and TIM23 (red) normalized to tubulin from CCCP-treated cells. Data were obtained from two independent experiments and are shown as means ± SD. (*E*) Parkin KO MEF cells expressing Myc-tagged Parkin WT or T415N were compared with Parkin WT MEF cells. Whole-cell lysates were analyzed for immunoblotting to detect indicated proteins. (*F*) Confocal images of Bax translocated to the mitochondria. HeLa cells were transfected with Myc-tagged Parkin WT or T415N and treated with 1 mM H_2O_2 for 6 h. Subcellular localizations of Bax (green), COXIV (blue), and Parkin (red) were examined by confocal microscopy. (Scale bars, 20 μm.) (*G*) Percentage of cells with Bax in mitochondria in *F* ($n > 450$ cells from three independent experiments). Data were analyzed by ANOVA Tukey test. $^{***}P < 0.001$

(Fig. 5*B* and *SI Appendix*, Fig. S8 *A–E*). Excitingly, T415N mutation in the R2 domain of Parkin abolished VDAC1 monoubiquitination but still retained its polyubiquitination activity (Fig. 5 *B* and *C*). Therefore, we decided to examine the effect of the Parkin T415N mutation on mitophagy and apoptosis.

To observe the effect of the Parkin T415N mutation on mitophagy, we analyzed the amount of mitochondrial proteins in HeLa cells expressing Parkin WT or T415N mutant using immunoblotting. The amount of mitochondrial proteins in the cells expressing Parkin WT and T415N generally decreased after CCCP treatment, confirming that Parkin-mediated mitophagy does occur normally in the Parkin T415N patient mutant (Fig. 5*D*). This was consistent with the results from the mammalian cells expressing VDAC1 deficient with monoubiquitination (VDAC1 K274R), indicating that Parkin with the T415N mutation does not affect mitophagy by specifically impairing VDAC1 monoubiquitination.

Next, we examined the occurrence of apoptosis by observing the amount of cleaved caspase3. When comparing Parkin WT and Parkin KO MEF cells, increased cleaved caspase3 was observed only in Parkin KO MEF cells (Fig. 5*E*). Furthermore, the increased cleaved caspase3 in Parkin KO MEF cells was effectively reduced by the expression of exogenous Parkin WT, but not by the Parkin T415N mutant (Fig. 5*E*). Finally, we observed Bax translocation to the mitochondria in order to determine the effect of the Parkin T415N mutation on apoptosis. When treated with 1 mM H_2O_2, cells expressing Parkin T415N displayed mitochondrial translocation of Bax protein (Fig. 5*F*). The quantification data showed that ∼30% of the cells expressing Parkin T415N had Bax localized to the mitochondria, whereas cells expressing Parkin WT had no difference in the translocation of Bax to the mitochondria compared to the control (Fig. 5*G*). Overall, these findings demonstrated that apoptosis can be induced in the cells expressing the Parkin T415N mutant, which is defective in inducing VDAC1 monoubiquitination.

***Drosophila* Parkin T433N, the Correspondent to the Human Parkin T415N Mutant, Induces PD Phenotypes.** To investigate the Parkin PD patient mutation with deficiency in VDAC1 monoubiquitination in vivo, we generated transgenic flies expressing *Drosophila* Parkin WT or T433N (T415N in human). The transgenic flies expressed equal amounts of Parkin proteins, as shown by IB analyses (*SI Appendix*, Fig. S4*B*). We examined whether Parkin null flies (*park*^{1}) displaying PD-related phenotypes could be rescued by the expression of exogenous Parkin WT or T433N.

Furthermore, we examined the mitochondria morphology and conducted TUNEL assays in the thoraces of *Drosophila*. As shown previously, *park*^{1} flies displayed abnormalities in mitochondrial morphology (Fig. 6 *A* and *B*) and increased thoracic TUNEL signals (Fig. 6 *A* and *B*), which correlate with their decreased climbing ability (Fig. 6*C*). When *park*^{1} flies were induced to express exogenous Parkin WT, the defective phenotypes of *park*^{1} flies were fully rescued (Fig. 6 *A–C*). However, the expression of exogenous Parkin T433N failed to rescue the defective phenotypes (Fig. 6 *A–C*). In addition, we measured the number of DA neurons in the PPL1 region of brain after inducing the expression of Parkin WT or T433N in the entire body using the *hs-gal4* driver. *park*^{1} flies showed a decrease in DA neurons in the PPL1 regions, as previously reported (37), which was rescued by the expression of exogenous Parkin WT but not by Parkin T433N (Fig. 6*D*). From these data, we concluded that the regulation of VDAC1 monoubiquitination by Parkin is important in protecting cells from apoptosis that may lead to PD pathogenesis.

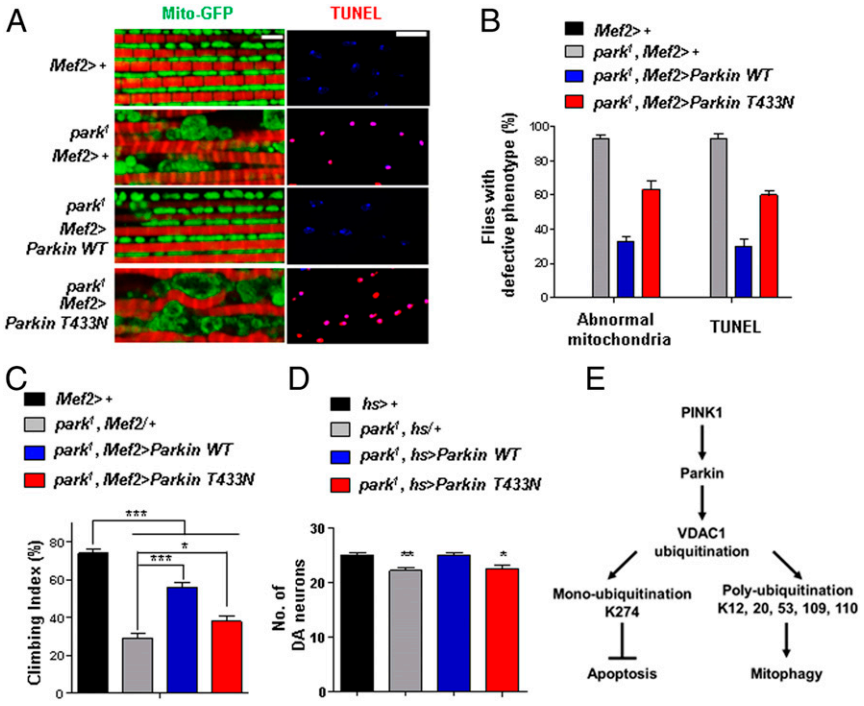

Fig. 6. *Drosophila* Parkin T433N cannot rescue the PD-related phenotypes of the *park*^{1} mutant. (*A*) Mitochondrial morphology and TUNEL signals in the thoraces of Parkin-null flies (*park*^{1}) expressing Parkin WT or T433N using the *Mef2-Gal4* driver. Mitochondrial morphology (green) and phalloidin staining (red) to indicate muscle fiber are shown (*Left*). TUNEL signals (red) and 4′,6-diamidino-2-phenylindole staining (blue) are shown (*Right*). (Scale bars, 5 μm.) (*B*) Percentage of flies with defective mitochondrial morphology or TUNEL signals (n = 100 from 10 independent experiments). (*C*) Percentage of flies with defective climbing ability (n = 100 from 10 independent experiments). (*D*) Numbers of DA neurons in the PPL1 region (n = 10). All quantifications were analyzed by one-way ANOVA with Tukey multiple-comparison test and are presented as means ± SD. *P < 0.05; **P < 0.01; ***P < 0.001. (*E*) A schematic model of mitophagy and apoptosis regulated by two types of ubiquitination on VDAC1 in the PINK1–Parkin pathway.

Discussion

In this study, we demonstrated that Parkin induces mono- and polyubiquitination on VDAC1 to regulate apoptosis and mitophagy, respectively (Fig. 6*E*). Interestingly, one of the PD patient mutations in Parkin, Parkin T415N, specifically fails to induce VDAC1 monoubiquitination and inhibit apoptosis, while it did not affect VDAC1 polyubiquitination and mitophagy. Using *Drosophila* models, we demonstrated that defects in Porin monoubiquitination induce phenotypes related to PD pathogenesis, such as increased apoptosis, decreased locomotive activities, defective mitochondrial morphology, and DA neurodegeneration, thus suggesting the importance of the tight regulation of VDAC1-mediated apoptosis in PD pathogenesis.

Although some have reported that VDAC1 is a critical component for the PINK1–Parkin pathway, others have argued that VDAC1 is irrelevant to mitophagy and doubted its role as a critical substrate of the PINK1–Parkin pathway. However, a recent paper has shown that VDAC1 is indeed one of the regulators of mitophagy (45). Using proteomics analyses, the authors showed that the lysine sites of 12, 20, 53, 109, 161, 266, and 274 on human VDAC1 are ubiquitinated upon the activation of PINK1 and Parkin. In our experiment, we also found that most of the lysine residues are proved to be the sites of ubiquitination by Parkin, more specifically monoubiquitination (K274) and polyubiquitination (K12, 20, 53, 109, and 110). Moreover, our data showed that the absence of VDAC1 polyubiquitination hinders the recruitment of Parkin to the mitochondria and subsequently impairs mitophagy, supporting the important roles of VDAC1 in mediating mitophagy induced by the PINK1–Parkin pathway.

The Parkin T415N mutation has been reported to have no defect in translocation to the mitochondria, but the ability of ubiquitinating substrates is reduced (46, 47). However, here we showed that Parkin T415N only inhibits monoubiquitination of VDAC1, suggesting an unknown mechanism for Parkin to differentially induce mono- and polyubiquitination on its substrates. Since there are several proteins ubiquitinated by Parkin and controlling apoptosis, such as PARIS, BAX, BAK, and BCL-2 (48–51), further studies are needed to understand their ubiquitination patterns and underlying molecular mechanisms for how Parkin induces different types of ubiquitination.

According to our results, VDAC1 monoubiquitination inhibits apoptosis and VDAC1 polyubiquitination promotes mitophagy, which means that the regulation of apoptosis and mitophagy by the PINK1–Parkin pathway occurs antagonistically via VDAC1. Consistently, previous data obtained by others showed that increased apoptosis often suppresses induction of autophagy. For instance, caspases that are activated in apoptotic processes cleave Beclin1, creating Beclin1 fragments to inhibit the binding of Vps34, thereby suppressing autophagy (52). Atg5, a major component in autophagy, is also cleaved by calpain in response to apoptotic stimuli (53). Moreover, knockdown of activating molecule in beclin1-regulated autophagy (AMBRA1), an autophagy regulator, has been shown to sensitize cells to apoptotic stimuli, and, additionally, when AMBRA1 is cleaved by caspases and degraded by calpain, autophagy is inactivated (54). These findings suggest that depending on the types and degrees of apoptotic stimuli, such as mitochondrial damages, the balance between mitophagy and apoptosis are induced against each other to determine cellular fates. Thus, we propose that under mitochondrial damages that promote mitophagy, both mono- and polyubiquitination of VDAC1 would increase to inhibit apoptosis. However, when apoptosis is triggered, both types of ubiquitination would be suppressed to induce apoptosis. Further investigations are required to validate this hypothesis.

Atomic force microscopy images of yeast VDAC (55, 56) and IB analyses of VDAC1 extracted from rat brain and liver tissues (57, 58) revealed that VDAC1 forms oligomeric structures. Furthermore, apoptotic signals induce VDAC1 oligomerization. Interestingly, a recent study identified the contact sites for the dimerization of VDAC1, which are necessary for VDAC1 to form self-oligomers (59). Replacing hydrophobic amino acids with charged ones in the beta-strands 1, 2, and 19 of VDAC1 interferes with VDAC1 oligomerization. We have identified that VDAC1 monoubiquitination occurs on the K274 position of beta-strand 19. Therefore, it may be possible that the monoubiquitination disturbs VDAC1 self-oligomerization, resulting in inhibition of apoptosis.

In this study, we also demonstrated that VDAC1 monoubiquitination regulates mitochondrial calcium influx. We showed that the loss of VDAC1 monoubiquitination leads to increased mitochondrial calcium influx and apoptosis. More importantly, we confirmed that calcium is a major contributor to the PD-related phenotypes of Porin mutant flies by rescuing VDAC1 K273R flies with knocking out MCU (Fig. 4 *A–F*). These data suggested that the regulation of mitochondrial calcium influx by VDAC1 monoubiquitination plays a critical role in inducing apoptosis and consequent PD pathogenesis.

In conclusion, we have identified a molecular target of the PINK1–Parkin pathway connected to PD pathogenesis, which is apoptotic regulation via VDAC1 monoubiquitination. We propose that the proper control of VDAC1 monoubiquitination could be a way to prevent and treat PD.

Materials and Methods

DNA Constructs and Reagents. WT VDAC1 plasmid was constructed into pcDNA3.1 zeo (+) N-terminal HA-tagged vector. VDAC1 mutants (K12R, K20R, K53R, K109R, K110R, K274R, and All-KR) and the 63 PD missense mutants of Parkin (Fig. 5*A* and *SI Appendix*, Fig. S8 *A–E*) were generated using a site-directed point mutagenesis method. N-terminal flag-tagged human ubiquitin was cloned into pcDNA3.1 vector. N-terminal GST-tagged pEBG vector and N-terminal Myc-tagged pcDNA3.1 zeo (+) vector were used to express Parkin constructs. The E3 ligase activity-dead mutant of Parkin, Parkin C431S, and other Parkin PD patient mutants were constructed through site-directed mutagenesis in either pEBG vector or Myc-tagged pcDNA3.1 zeo (+) vector. Flag-tagged mouse Bax was also cloned into pcDNA3.1 zeo (+) vector or pGFPC1 vector. YFP-Parkin was purchased from Addgene (no. 23955). Cells were treated with CCCP (Sigma), Ru360 (Calbiochem), and transfected human MCU siRNA (nos. 90550-1 and 90550-2; Bioneer).

Cell Culture and Transfection. HEK293T, HeLa cells, VDAC1 WT and KO MEF, and Parkin WT or KO MEF cells were cultured in Dulbecco Modified Eagle Medium (DMEM) (Welgene) supplemented with 10% fetal bovine serum (FBS) (Invitrogen) at 37 °C in a humidified atmosphere composed of 5% CO_2. HeLa cells stably expressing GFP-tagged Parkin were cultured in advanced DMEM (Invitrogen) with 10% FBS (Invitrogen), 5 μg/mL puromycin (Invitrogen), and 200 mM L-glutamine (Invitrogen) at 37 °C in a humidified atmosphere composed of 5% CO_2. HEK293T cells were transfected using polyethylenimine (PEI) reagent (Sigma). HeLa and GFP-Parkin–expressing HeLa cells were transfected using Lipofectamine LTX (Invitrogen), and MEF cells were transfected using Lipofectamine 3000 (Invitrogen) as instructed by the manufacturer.

Antibodies. For IB and immunofluorescence (IF) analyses, the following antibodies were used: rabbit anti-HA (IB, 1:1,000; IF, 1:200; Cell Signaling), mouse anti-Flag (IB, 1:1,000; IF, 1:200; MBL), rabbit anti-ubiquitin (IB, 1:1,000; Cell Signaling), mouse anti-GST (IB, 1:1,000; Upstate), mouse anti-Myc (IB, 1:1,000; MBL), rabbit anti-p62/SQSTM1 (IF, 1:200; Cell Signaling), rabbit anti-MFN1 (IB, 1:1,000; Abcam), mouse anti-MFN2 (IB, 1:1,000; Abcam), rabbit anti-COXIV (IB, 1:1,000; Abcam), mouse anti-TIM23 (IB, 1:1,000; BD Sciences), mouse anti-NDUFS3 (IB, 1:1,000; Abcam), mouse anti-MnSOD (IB, 1:1,000; BD Sciences), mouse anti-tubulin (IB, 1:1,000; E7 clone; Developmental Studies Hybridoma Bank), rabbit anti-cleaved PARP (IB, 1:1,000; Cell Signaling), and rabbit anti-cleaved caspase3 (IB, 1:1,000; Cell Signaling). Peroxidase-conjugated secondary antibodies, mouse anti-tetramethylrhodamine (TRITC) antibody, rabbit anti-TRITC antibody, mouse anti-fluorescein isothiocyanate antibody, and rabbit anti-Alexa Fluor647 antibodies were purchased from The Jackson Laboratory.

Immunofluorescence. HeLa cells, HeLa cells stably expressing GFP-Parkin, and MEF cell lines were subcultured on coverslips in 12-well tissue culture plates. Cells were treated with 20 μM CCCP or dimethyl sulfoxide (DMSO), fixed in

4% paraformaldehyde (PFA) for 15 min, and permeabilized with 0.5% Triton X-100 in phosphate-buffered saline (PBS-T) for 5 min. For the staining of p62/SQSTM1, cells were permeabilized with ice-cold 100% methanol for 20 min, and then the cells were incubated in blocking solution (4% bovine serum albumin [BSA] and 1% normal goat serum in PBS-T) for 1 h at room temperature. Primary antibodies were added to blocking solution and the cells were incubated overnight at 4 °C. After washing with PBS-T (0.1% Triton X-100 in PBS) for four times, cells were incubated in the blocking solution with secondary antibodies for 1 h at room temperature. The antibody-labeled cells were then washed with PBS-T (0.1% Triton X-100 in PBS) for six times and were mounted with mounting solution (100 mg/mL 1,4-diazabicyclo [2.2.2] octane in 90% glycerol). The prepared slides were observed under LSM710 laser scanning confocal microscope (Carl Zeiss). All immunostaining experiments with HeLa cells were conducted at least three times ($n > 150$). For analysis of Bax translocation to the mitochondria, we counted cells in which Bax is colocalized with VDAC1 in the mitochondria. For quantification analysis, we used the Image J program.

Immunoprecipitation and Immunoblotting. For immunoprecipitation, cells were lysed using a lysis buffer A—20 mM tris(hydroxymethyl)aminomethane (Tris) (pH 7.5), 100 mM NaCl, 1 mM ethylenediaminetetraacetic acid, 2 mM egtazic acid, 50 mM β-glycerophosphate, 50 mM NaF, 1 mM sodium vanadate, 2 mM dithiothreitol (DTT), 1 mM phenylmethylsulfonyl fluoride (PMSF), 10 g/mL leupeptin, 1 g/mL pepstatin A, and 1% Triton X-100—and were subjected to immunoprecipitation and immunoblotting according to standard procedures. Cell lysates were centrifuged at 13,000 rpm at 4 °C for 15 min and were incubated overnight after the addition of primary antibodies. Lysates were then incubated with protein A/G agarose beads for 2 h at 4 °C, washed three times in detergent-free lysis buffer A, and eluted with 2× Laemmli buffer at 95 °C. IB analyses for mitochondrial proteins were performed using radioimmunoprecipitation assay buffer (50 mM Tris pH 8.0, 150 mM NaCl, 0.5% sodium deoxycholate, 1% Nonidet P-40, 0.1% sodium dodecyl sulfate (SDS), 2 mM DTT, 1 mM PMSF, 10 g/mL leupeptin, and 1 g/mL pepstatin A). Total proteins were quantified using the BCA protein assay kit (Pierce). Lysates were subjected to SDS/polyacrylamide gel electrophoresis analysis followed by immunoblotting according to standard procedures. The blots were developed and viewed under LAS4000 (Fujifilm).

Calcium Measurement in Cells. VDAC1 WT and KO MEF or Parkin WT and KO MEF cell lines were transfected with a mitochondrial calcium indicator 4mitD3 (458 nm excitation/470- to 500-nm and 530- to 560-nm emission; provided by Kyu-Sang Park, Yonsei University Wonju Medical School, Wonju, Republic of Korea), using Lipofectamine 3000. After 48 h of transfection, we monitored living cells expressing 4mitD3 using LSM710 confocal microscopy. During the monitoring process, cells were perfused with KRB solution (140 mM NaCl, 3.6 mM KCl, 0.5 mM NaH_2PO_4, 0.5 mM $MgSO_4$, 1.5 mM $CaCl_2$, 10 mM Hepes, 2 mM $NaHCO_3$, and 5.5 mM glucose and pH 7.4-titrated with NaOH) and treated with 100 μM adenosine triphosphate (ATP) for 3 min. The ratio fluorescence responses (530 to 560 nm/470 to 500 nm) were observed using a LSM710 laser scanning confocal microscope (Carl Zeiss).

Statistical Analysis. Statistical analyses were performed appropriately using ANOVA Tukey test and are presented as means ± SD.

Fly Stocks. The *Drosophila* lines used in the experiments were *Mef2-Gal4* (no. 27390; Bloomington Drosophila Stock Center), *TH-gal4* (stock no. 8848; Bloomington Drosophila Stock Center), *hs-gal4* (no. 2077; Bloomington Drosophila Stock Center), *UAS-MitoGFP* (60), *MCUΔ52* (61), *park*^{1} (no. 34747; Bloomington Drosophila Stock Center), *UAS-Porin WT-Flag* (44), and *UAS-Myc-Parkin* (44). *pUAST-Porin K273R-Flag* and *pUAST-Porin Poly-KR-Flag* were generated by mutating *pUAST-Porin WT-Flag* (cg6647) and were microinjected into *w*^{1118} embryos. *pUAST-Myc-Parkin T433N* was generated by mutating *pUAST-Myc-Parkin WT* and was microinjected into *w*^{1118} embryos. All flies were grown in standard cornmeal–yeast–agar medium at 25 °C.

Quantification of the Wing Phenotypes of Flies. For quantification, wing phenotypes of 3-d-old female flies were examined ($n > 100$).

Behavioral Assays. The climbing index refers to the percentage of flies that climb above 15 cm in 12 s from climbing assays. For the *Drosophila* climbing assay, ten 3-d-old female flies were transferred into 18-cm-long vials and were incubated for 5 min at room temperature for environmental acclimatization. After tapping down flies to the bottom of vial, the percentage of flies arriving at the 15 cm high finish line within 12 s was measured. Ten trials were performed per group, and the assay was repeated with 10 different groups.

Muscle Dissection and Mitochondrial Staining. For streptavidin staining to detect mitochondria, the head of each fly was surgically removed and the body was fixed in 4% PFA for 1 h at room temperature. After fixation, thoraces were vertically cut in half by dissecting along the bristles in the middle of the thorax and then washed with PBS-T (0.1% Triton X-100 in PBS). The samples were blocked for 30 min at room temperature with PBS-T containing 3% BSA. Next, samples were incubated at 4 °C for 16 h with Alexa 488-conjugated streptavidin (Invitrogen) for mitochondria staining and with TRITC-phalloidine (Sigma) for muscle fiber staining. The samples were finally washed with PBS-T and were mounted in 80% glycerol-PBS solution to be observed under an LSM710 confocal microscope. For quantification, a fly having a mitochondrion with a length over 5 μm and a width over 3.5 μm was defined as a fly having swollen mitochondria. Ten 3-d-old female flies were observed as 1 group, and 10 groups of each genotype were examined.

Tyrosine Hydroxylase Immunostaining and Quantification of DA Neurons. 30-d-old adult fly brains were fixed with 4% PFA and stained with anti-tyrosine hydroxylase (TH) antibody, as described in previous research (37). The samples were observed and imaged by an LSM710 confocal microscope (Carl Zeiss). To quantify DA neurons, the PPL1 of 10 fly brains from each genotype was observed.

TUNEL Assay. Dissected 3-d-old female fly thoraces were fixed with 4% PFA and washed with PBS. Samples were incubated in 0.1 M sodium citrate dissolved in PBS at 65 °C, and apoptotic cells were detected using an in situ cell death detection kit. After TUNEL reaction, samples were stained with Hoechst 33258 (Invitrogen) to detect nuclei. For quantification, TUNEL signals of ten 3-d-old female flies were observed. A fly having over 10 TUNEL dots in any of the 6 dorsal longitudinal muscles of indirect flight muscles was defined as a fly showing apoptotic signals, and the percentage of flies showing apoptotic signals was measured.

Data Availability. All data are available within this paper and the associated *SI Appendix*.

ACKNOWLEDGMENTS. We thank Kei Okatsu (Tokyo Metropolitan Institute of Medical Science) for HeLa cells stably expressing GFP-Parkin. VDAC1 WT or KO MEF cells were obtained from Geert Bultynck (KU Leuven University) and William Craigen (Baylor College of Medicine). Parkin WT or KO MEF cells were provided by Hodaka Yamakado (Kyoto University Graduate School of Medicine). J.C. was supported by Grant HI17C0328 from the Korea Health Technology Research and Development Project, through the Korea Health Industry Development Institute, funded by the Ministry of Health and Welfare (2010-0018291). S.J.H., D.L., H.Y., K.J., and J.C. were supported by BK21 Plus Program from the Ministry of Education, Republic of Korea. S.J.H. was supported by National Research Foundation of Korea Grant NRF-2019R1I1A1A01061717.

1. Y. Baba *et al.*, Phenotypic commonalities in familial and sporadic Parkinson disease. *Arch. Neurol.* **63**, 579–583 (2006).
2. V. Bonifati *et al.*, Mutations in the DJ-1 gene associated with autosomal recessive early-onset parkinsonism. *Science* **299**, 256–259 (2003).
3. S. Hague *et al.*, Early-onset Parkinson's disease caused by a compound heterozygous DJ-1 mutation. *Ann. Neurol.* **54**, 271–274 (2003).
4. Y. Hatano *et al.*, Novel PINK1 mutations in early-onset parkinsonism. *Ann. Neurol.* **56**, 424–427 (2004).
5. T. Kitada *et al.*, Mutations in the parkin gene cause autosomal recessive juvenile parkinsonism. *Nature* **392**, 605–608 (1998).
6. M. H. Polymeropoulos *et al.*, Mutation in the alpha-synuclein gene identified in families with Parkinson's disease. *Science* **276**, 2045–2047 (1997).
7. E. M. Valente *et al.*, Hereditary early-onset Parkinson's disease caused by mutations in PINK1. *Science* **304**, 1158–1160 (2004).
8. C. Kondapalli *et al.*, PINK1 is activated by mitochondrial membrane potential depolarization and stimulates Parkin E3 ligase activity by phosphorylating Serine 65. *Open Biol.* **2**, 120080 (2012).
9. S. J. Ham *et al.*, Interaction between RING1 (R1) and the ubiquitin-like (UBL) domains is critical for the regulation of Parkin activity. *J. Biol. Chem.* **291**, 1803–1816 (2016).
10. N. Matsuda *et al.*, PINK1 stabilized by mitochondrial depolarization recruits Parkin to damaged mitochondria and activates latent Parkin for mitophagy. *J. Cell Biol.* **189**, 211–221 (2010).
11. D. P. Narendra *et al.*, PINK1 is selectively stabilized on impaired mitochondria to activate Parkin. *PLoS Biol.* **8**, e1000298 (2010).

12. K. Okatsu *et al*., PINK1 autophosphorylation upon membrane potential dissipation is essential for Parkin recruitment to damaged mitochondria. *Nat. Commun.* **3**, 1016 (2012).
13. S. A. Sarraf *et al*., Landscape of the PARKIN-dependent ubiquitylome in response to mitochondrial depolarization. *Nature* **496**, 372–376 (2013).
14. X. Wang *et al*., PINK1 and Parkin target Miro for phosphorylation and degradation to arrest mitochondrial motility. *Cell* **147**, 893–906 (2011).
15. S. M. Yoo, Y. K. Jung, A molecular approach to mitophagy and mitochondrial dynamics. *Mol. Cells* **41**, 18–26 (2018).
16. M. Bayrhuber *et al*., Structure of the human voltage-dependent anion channel. *Proc. Natl. Acad. Sci. U.S.A.* **105**, 15370–15375 (2008).
17. C. P. Baines *et al*., Loss of cyclophilin D reveals a critical role for mitochondrial permeability transition in cell death. *Nature* **434**, 658–662 (2005).
18. C. P. Baines, R. A. Kaiser, T. Sheiko, W. J. Craigen, J. D. Molkentin, Voltage-dependent anion channels are dispensable for mitochondrial-dependent cell death. *Nat. Cell Biol.* **9**, 550–555 (2007).
19. E. Basso *et al*., Properties of the permeability transition pore in mitochondria devoid of cyclophilin D. *J. Biol. Chem.* **280**, 18558–18561 (2005).
20. A. S. Belzacq, H. L. Vieira, G. Kroemer, C. Brenner, The adenine nucleotide translocator in apoptosis. *Biochimie* **84**, 167–176 (2002).
21. M. Crompton, The mitochondrial permeability transition pore and its role in cell death. *Biochem. J.* **341**, 233–249 (1999).
22. V. Shoshan-Barmatz, A. Israelson, D. Brdiczka, S. S. Sheu, The voltage-dependent anion channel (VDAC): Function in intracellular signalling, cell life and cell death. *Curr. Pharm. Des.* **12**, 2249–2270 (2006).
23. S. Geisler *et al*., PINK1/Parkin-mediated mitophagy is dependent on VDAC1 and p62/SQSTM1. *Nat. Cell Biol.* **12**, 119–131 (2010).
24. S. Abu-Hamad, H. Zaid, A. Israelson, E. Nahon, V. Shoshan-Barmatz, Hexokinase-I protection against apoptotic cell death is mediated via interaction with the voltage-dependent anion channel-1: Mapping the site of binding. *J. Biol. Chem.* **283**, 13482–13490 (2008).
25. J. G. Pastorino, N. Shulga, J. B. Hoek, Mitochondrial binding of hexokinase II inhibits Bax-induced cytochrome c release and apoptosis. *J. Biol. Chem.* **277**, 7610–7618 (2002).
26. S. Shimizu, M. Narita, Y. Tsujimoto, Bcl-2 family proteins regulate the release of apoptogenic cytochrome c by the mitochondrial channel VDAC. *Nature* **399**, 483–487 (1999).
27. S. Shimizu, A. Konishi, T. Kodama, Y. Tsujimoto, BH4 domain of antiapoptotic Bcl-2 family members closes voltage-dependent anion channel and inhibits apoptotic mitochondrial changes and cell death. *Proc. Natl. Acad. Sci. U.S.A.* **97**, 3100–3105 (2000).
28. S. Shimizu, Y. Matsuoka, Y. Shinohara, Y. Yoneda, Y. Tsujimoto, Essential role of voltage-dependent anion channel in various forms of apoptosis in mammalian cells. *J. Cell Biol.* **152**, 237–250 (2001).
29. S. Shimizu, T. Ide, T. Yanagida, Y. Tsujimoto, Electrophysiological study of a novel large pore formed by Bax and the voltage-dependent anion channel that is permeable to cytochrome c. *J. Biol. Chem.* **275**, 12321–12325 (2000).
30. N. Keinan, D. Tyomkin, V. Shoshan-Barmatz, Oligomerization of the mitochondrial protein voltage-dependent anion channel is coupled to the induction of apoptosis. *Mol. Cell. Biol.* **30**, 5698–5709 (2010).
31. G. Szabadkai *et al*., Chaperone-mediated coupling of endoplasmic reticulum and mitochondrial Ca2+ channels. *J. Cell Biol.* **175**, 901–911 (2006).
32. Y. Liao *et al*., Mitochondrial calcium uniporter protein MCU is involved in oxidative stress-induced cell death. *Protein Cell* **6**, 434–442 (2015).
33. E. Doran, A. P. Halestrap, Cytochrome c release from isolated rat liver mitochondria can occur independently of outer-membrane rupture: Possible role of contact sites. *Biochem. J.* **348**, 343–350 (2000).
34. J. M. Heo, A. Ordureau, J. A. Paulo, J. Rinehart, J. W. Harper, The PINK1-PARKIN mitochondrial ubiquitylation pathway drives a program of OPTN/NDP52 recruitment and TBK1 activation to promote mitophagy. *Mol. Cell* **60**, 7–20 (2015).
35. J. Shi *et al*., NBR1 is dispensable for PARK2-mediated mitophagy regardless of the presence or absence of SQSTM1. *Cell Death Dis.* **6**, e1943 (2015).
36. Y. C. Wong, E. L. Holzbaur, Optineurin is an autophagy receptor for damaged mitochondria in parkin-mediated mitophagy that is disrupted by an ALS-linked mutation. *Proc. Natl. Acad. Sci. U.S.A.* **111**, E4439–E4448 (2014).
37. J. Park *et al*., Mitochondrial dysfunction in Drosophila PINK1 mutants is complemented by parkin. *Nature* **441**, 1157–1161 (2006).
38. B. Antonsson, S. Montessuit, B. Sanchez, J. C. Martinou, Bax is present as a high molecular weight oligomer/complex in the mitochondrial membrane of apoptotic cells. *J. Biol. Chem.* **276**, 11615–11623 (2001).
39. K. G. Wolter *et al*., Movement of Bax from the cytosol to mitochondria during apoptosis. *J. Cell Biol.* **139**, 1281–1292 (1997).
40. P. F. Cartron, L. Oliver, E. Mayat, K. Meflah, F. M. Vallette, Impact of pH on Bax alpha conformation, oligomerisation and mitochondrial integration. *FEBS Lett.* **578**, 41–46 (2004).
41. K. Janssen, S. Pohlmann, R. U. Jänicke, K. Schulze-Osthoff, U. Fischer, Apaf-1 and caspase-9 deficiency prevents apoptosis in a Bax-controlled pathway and promotes clonogenic survival during paclitaxel treatment. *Blood* **110**, 3662–3672 (2007).
42. J. Pawlowski, A. S. Kraft, Bax-induced apoptotic cell death. *Proc. Natl. Acad. Sci. U.S.A.* **97**, 529–531 (2000).
43. A. P. Halestrap, What is the mitochondrial permeability transition pore? *J. Mol. Cell. Cardiol.* **46**, 821–831 (2009).
44. J. Park *et al*., Drosophila Porin/VDAC affects mitochondrial morphology. *PLoS One* **5**, e13151 (2010).
45. A. Ordureau *et al*., Dynamics of PARKIN-dependent mitochondrial ubiquitylation in induced neurons and model systems revealed by digital snapshot proteomics. *Mol. Cell* **70**, 211–227.e8 (2018).
46. J. Y. Lee, Y. Nagano, J. P. Taylor, K. L. Lim, T. P. Yao, Disease-causing mutations in parkin impair mitochondrial ubiquitination, aggregation, and HDAC6-dependent mitophagy. *J. Cell Biol.* **189**, 671–679 (2010).
47. K. Okatsu *et al*., p62/SQSTM1 cooperates with Parkin for perinuclear clustering of depolarized mitochondria. *Genes Cells* **15**, 887–900 (2010).
48. Y. Lee *et al*., PINK1 primes Parkin-mediated ubiquitination of PARIS in dopaminergic neuronal survival. *Cell Rep.* **18**, 918–932 (2017).
49. B. N. Johnson, A. K. Berger, G. P. Cortese, M. J. Lavoie, The ubiquitin E3 ligase parkin regulates the proapoptotic function of Bax. *Proc. Natl. Acad. Sci. U.S.A.* **109**, 6283–6288 (2012).
50. J. P. Bernardini *et al*., Parkin inhibits BAK and BAX apoptotic function by distinct mechanisms during mitophagy. *EMBO J.* **38**, e99916 (2019).
51. D. Chen *et al*., Parkin mono-ubiquitinates Bcl-2 and regulates autophagy. *J. Biol. Chem.* **285**, 38214–38223 (2010).
52. S. Luo, D. C. Rubinsztein, Apoptosis blocks beclin 1-dependent autophagosome synthesis: An effect rescued by Bcl-xL. *Cell Death Differ.* **17**, 268–277 (2010).
53. S. Yousefi *et al*., Calpain-mediated cleavage of Atg5 switches autophagy to apoptosis. *Nat. Cell Biol.* **8**, 1124–1132 (2006).
54. V. Pagliarini *et al*., Proteolysis of Ambra1 during apoptosis has a role in the inhibition of the autophagic pro-survival response. *Cell Death Differ.* **19**, 1495–1504 (2012).
55. R. P. Gonçalves, N. Buzhynskyy, V. Prima, J. N. Sturgis, S. Scheuring, Supramolecular assembly of VDAC in native mitochondrial outer membranes. *J. Mol. Biol.* **369**, 413–418 (2007).
56. B. W. Hoogenboom, K. Suda, A. Engel, D. Fotiadis, The supramolecular assemblies of voltage-dependent anion channels in the native membrane. *J. Mol. Biol.* **370**, 246–255 (2007).
57. V. Shoshan-Barmatz, R. Zalk, D. Gincel, N. Vardi, Subcellular localization of VDAC in mitochondria and ER in the cerebellum. *Biochim. Biophys. Acta* **1657**, 105–114 (2004).
58. R. Zalk, A. Israelson, E. S. Garty, H. Azoulay-Zohar, V. Shoshan-Barmatz, Oligomeric states of the voltage-dependent anion channel and cytochrome c release from mitochondria. *Biochem. J.* **386**, 73–83 (2005).
59. S. Geula, H. Naveed, J. Liang, V. Shoshan-Barmatz, Structure-based analysis of VDAC1 protein: Defining oligomer contact sites. *J. Biol. Chem.* **287**, 2179–2190 (2012).
60. A. D. Pilling, D. Horiuchi, C. M. Lively, W. M. Saxton, Kinesin-1 and Dynein are the primary motors for fast transport of mitochondria in Drosophila motor axons. *Mol. Biol. Cell* **17**, 2057–2068 (2006).
61. S. Choi *et al*., Mitochondrial calcium uniporter in *Drosophila* transfers calcium between the endoplasmic reticulum and mitochondria in oxidative stress-induced cell death. *J. Biol. Chem.* **292**, 14473–14485 (2017).